Epidemic models with restricted circulation and social distancing on some network topologies*

Álvaro Junio Pereira Franco[1][0000−0002−7602−0599]

Federal University of Santa Catarina, Technological Center
Department of Informatics and Statistics, Florianópolis SC, Brazil
alvaro.junio@ufsc.br

Abstract. A model to simulate the spreading of a disease on a network is proposed. The SIS and SIR models, a social distancing factor and network circulation restrictions are considered. We perform some experiments that give us an idea of how a disease spreads on different network topologies and social distancing factors.

Keywords: Epidemic models · Networks · Simulations

1 Introduction

Nowadays we are witnessing a pandemic. The health system and the economy of the region affected by a disease can suffer serious damage without proposals to control its spreading. So, control policies to lead this spreading are necessary. The ideal is that public agents and society together act quickly applying policies as fast as they can to avoid that a disease reaches people and advances on territory.

Follow the real numbers of infected people, recovered people, and the real number of occupied and empty beds in hospitals are important statistics in combat to pandemic. Other important question is the possibility to estimate with quality such numbers given some initial conditions. Hethcote [5] describes three fundamental epidemiological mathematical models which are used to follow the dynamic of a disease. The models classify people in groups and they depend on the following scenario: 1. a person is subject to contract a disease even if he (she) was already cured; 2. a person is subject to contract a disease, however, if he (she) contracted it in the past and he (she) is now cured then he (she) cannot contract the disease again; 3. a healthy person can be immune or can be vaccinated, thus avoiding to contract a disease. In the first scenario, we have the model named SIS. In this model people are classify as *susceptible* (those that are subject to contract a disease) and *infected* (those with a disease). In the second scenario, we have the SIR model. In this case, people are classify as susceptible, infected and *recovered* (those that were infected and will not be infected anymore). The recovered class can include dead people. In the third scenario, the SIRV model, people are classify as susceptible, infected, recovered and vaccinated.

* Supported by CNPq Proc. 423833/2018-9

It is common to find ordinary differential equations models to simulate the dynamic of a disease and to estimate the numbers of susceptible, infected, recovered and vaccinated people over time. A classic epidemiological model which uses differential equations is the Kermack and McKendrick model [6]. In their work, they consider the groups of people that are susceptible, infected and recovered. The Linge and Langtangen' book [7] have a section dedicated to the treatment of spreading disease through the numerical solution of ordinary differential equations.

Other models use cellular automata to study the spatial effects of an epidemic. White, del Rey and Sánchez [10] introduced a cellular automata model to simulate the epidemic spreading. Beauchemin, Samuel, and Tuszynski [3] used cellular automata to study the influenza A spreading. There are other works on this subject such as [1], [11] and [8].

This work follows the same way of the models based on cellular automata. Here we study the disease effect in a *generalized automata network* [9] with different *topologies*. We focus on two points whose turn more difficult the disease spreading by the network: the *circulation restrictions* transforming a real network topology to a particular network topology, providing a network strongly structured; and the *social distancing* through the possibility of people answer positively requests from public agent, media, academy, etc. We perform experiments on the SIR model and illustrate its characteristic graphics on different network topologies and in different social distancing levels.

To finish this section, we describe how this work is organized. In Section 2, we start with the application of SIS model in a network. In Section 3, we describe how we treat the social distancing. In this work, we suppose that a disease is spread by the contact between two people, a susceptible and an infected. So, in Section 4, we add to the model the rule of encounter among people. Section 5 considers the SIR model in a network. In Section 6, we analyze the experimental results on some network topologies.

2 The SIS model and the generalized automata network

The SIS model supposes, for each time t, a set of infected people I^t and a set of susceptible people S^t. The people set maintains constant $N^t = I^t \cup S^t$. A susceptible person on time t can become infected on time $t+1$ and vice versa. We know that a susceptible person becomes infected when he (she) has a contact with the disease virus. However, in this work we concentrate the infections occurring in the contact of a susceptible person and an infected person. There is a *virulence rate* $v \in [0, 1]$ that represents the potential infection of a contact. A *recovered rate* of infected people from the time t to $t+1$, $\varepsilon \in [0, 1]$, is also considered. Next it is given a simple model to estimate the number of susceptible and infected people for each time t

$$|I^t| = |I^{t-1}| - \varepsilon|I^{t-1}| + v|X^{t-1}|,$$
$$|S^t| = |S^{t-1}| - v|X^{t-1}| + \varepsilon|I^{t-1}|$$

where X^{t-1} is the set of people $p \in S^{t-1}$ that have encountered with some infected person. Note that $|N^t| = |I^t| + |S^t| = |I^{t-1}| - \varepsilon|I^{t-1}| + v|X^{t-1}| + |S^{t-1}| - v|X^{t-1}| + \varepsilon|I^{t-1}| = |N^{t-1}|$. Therefore, the model maintains the total number of people constant over time. For a while, we allow $|I^t|$ and $|S^t|$ be real numbers. Since this not reflect the reality of the world, in the following sections, we will keep these numbers as integer numbers.

We use generalized automata networks [9] to simulate the spreading of a disease. These type of automata extend *cellular automata* mainly changing their topologies. In cellular automata, the topology is given by a *regular lattice*. In generalized automata networks, the topology depends on a network. In this work, the network is used to represent the proximity among people. Consider a network $G = (V, E)$. The vertex set is formed by $V = \{1, 2, \ldots, n\}$. The edge set is formed by $E = \{\{i, j\} : i \text{ is adjacent to } j\}$. The set of vertices adjacent to vertex i is denoted by $\chi(i)$. A real value in interval $[0, 1]$ is associated to each vertex i, and it represents the social distancing factor of vertex i. Additionally, a group of people is associated to each vertex (people from the same neighborhood, same city, etc). They can be susceptible or infected. A certain proportion from these people answer to social distancing. Two vertices are adjacents if the two people groups have some proximity (neighborhoods or cities sharing a frontier). In this way, the generalized automata network can be used to simulate, for each time, the dynamic of susceptible and infected sets in each vertex. The group of people in a vertex i and on time t is denoted by the set $N_i^t = S_i^t \cup I_i^t$ (the intersection $S_i^t \cap I_i^t$ is empty). The number of elements in the sets S_i^t and I_i^t can vary over time, however, there is no removal in N_i^t. Although the graph structure is static, the number of susceptible, the number of infected people and the social distancing factor can be changed over time. Next sections, we describe how the distancing factor is considered and how the local interaction automata rule is defined.

3 The social distancing factor in the model

As previously described, each vertex has a real value associated to it, denoted by α_i^t, and representing the social distancing factor of people in vertex i and time t. The social distancing factor partitions the sets of people in two sets: those people that answer to social distancing and those that do not answer. The people that do not answer the distancing could go out its vertex and could keep going through the network. However, in our experiments, a person can stay in his (her) own vertex or can go through adjacent vertices. Therefore, the local interaction automata rule on vertex v depends of v itself and its adjacent vertices.

Now we add to the model the social distancing factor. We denote by $\dot{S}_i^t \subseteq S_i^t$ ($\ddot{S}_i^t \subseteq S_i^t$) the set of susceptible people in N_i^t that answer (do not answer) to social distancing. The set denoted by $\dot{I}_i^t \subseteq I_i^t$ ($\ddot{I}_i^t \subseteq I_i^t$) is the set of infected people that answer (do not answer) to social distancing. We will assume that the social distancing factor of each vertex i on time t, α_i^t, is applied equally on the sets S_i^t and I_i^t, that is, $|\dot{S}_i^t| = \lfloor \alpha_i^t |S_i^t| \rfloor$, $|\ddot{S}_i^t| = |S_i^t| - |\dot{S}_i^t|$, $|\dot{I}_i^t| = \lfloor \alpha_i^t |I_i^t| \rfloor$ and $|\ddot{I}_i^t| = |I_i^t| - |\dot{I}_i^t|$ (the function $\lfloor x \rfloor$ takes the integer part of x). Therefore,

we will have, for each time t, the set of people from N_i^t that answer to social distancing $\dot{N}_i^t = \dot{S}_i^t \cup \dot{I}_i^t$; and the set of people from N_i^t that do not answer to social distancing $\ddot{N}_i^t = \ddot{S}_i^t \cup \ddot{I}_i^t$. Next section, we detail how the local rule treats the contact between susceptible and infected people.

4 The local rule and the contact between people

In our scenario, for each time t, some people that answer to social distancing ($\lfloor \lambda_{\dot{S}} | \dot{S}_i^t | \rfloor$ and $\lfloor \lambda_{\dot{I}} | \dot{I}_i^t | \rfloor$) can be infected. This happens due to situations that require a person having to go out home (he (she) goes to drugstore, supermarket, etc). For the people that do not answer to social distancing, all the population ($\ddot{S}_i^t$) can become infected (on his (her) own vertex or in some adjacent). Therefore, for each vertex i, we can have people circling in i coming from the set N_i^t and from the set $\bigcup_{j \in \chi(i)} \ddot{N}_j^t$. Given such observation, it is important to us know the total number of people that are circling in each vertex of the network and in each time. This can be estimated by a tool that identifies the number of people in regions such that parks, shopping malls, workplaces, residences, transit, etc. Note that, it is not required the position where each person is but a *community mobility report*, such as in [4], giving the total number of people located in regions for each considered time.

Moreover, we can use a factor to represent the proportion of people which are circling in vertex i coming from vertex $j \in \chi(i)$ for each time t, here denoted by $\beta_{j \to i}^t$. Note that each edge $\{i, j\}$ may have two different factor $\beta_{i \to j}^t$ and $\beta_{j \to i}^t$, both are in the interval $[0, 1]$. Note also that the $\sum_{j \in \chi(i)} \beta_{i \to j}^t \leq 1$ for all vertex i and time t. For the case where the summation is strictly less than 1, then this gap means that some people stay in its own vertex. The experiments performed by this work consider $\beta_{i \to j}^t = \frac{1}{\chi(i)+1}$ for all vertex i, vertex $j \in \chi(i)$ and time t. So, the proportion of people that go out each vertex is *equally distributed* among the vertex itself and its adjacents. The Table 1 contain all variables representing circling people in vertex i for general and experiment cases.

Now, we give a description for the people circling in the network, for the experiment case (Table 1). The values in the first two lines represent the people that answer the distancing but, for some unavoidable reason, they have to go out home. From the next two lines in the table we know that people in vertex i that do not answer the distancing are distributed in their own vertex and in adjacent vertices; possibly, vertex i has more people (the rest of division). The two last lines show that each vertex receives from its adjacents an amount equally distributed. Note that a similar description can be given for the general case. Now, let us denote by $\dot{\mathcal{N}}_i^t = \dot{\mathcal{S}}_i^t + \dot{\mathcal{I}}_i^t$, by $\ddot{\mathcal{N}}_i^t = \ddot{\mathcal{S}}_i^t + \ddot{\mathcal{I}}_i^t$ and by $\dddot{\mathcal{N}}_i^t = \dddot{\mathcal{S}}_i^t + \dddot{\mathcal{I}}_i^t$.

In the model presented in Section 2, we denote by X^t the set of susceptible people that encountered an infected person on time t. Now, we consider the distancing factor. Denoted by $\dot{X}_i^t$ ($\ddot{X}_i^t$) the set of people from $p \in \dot{S}_i^t$ ($p \in \ddot{S}_i^t$) that encountered an infected person in vertex i (in adjacent vertices of i). The set of people $p \in S_i^t$ that encountered infected people is denoted by $X_i^t = \dot{X}_i^t \cup \ddot{X}_i^t$.

General case	Experiment case
$\dot{\mathcal{S}}_i^t : \lambda_{\dot{S}}\lvert\dot{S}_i^t\rvert$	$\lfloor\lambda_{\dot{S}}\lvert\dot{S}_i^t\rvert\rfloor$
$\dot{\mathcal{I}}_i^t : \lambda_{\dot{I}}\lvert\dot{I}_i^t\rvert$	$\lfloor\lambda_{\dot{I}}\lvert\dot{I}_i^t\rvert\rfloor$
$\ddot{\mathcal{S}}_i^t : \lvert\ddot{S}_i^t\rvert(1-\sum_{j\in\chi(i)}\beta_{i\to j}^t)$	$\left\lfloor\frac{\lvert\ddot{S}_i^t\rvert}{\lvert\chi(i)\rvert+1}\right\rfloor + (\lvert\ddot{S}_i^t\rvert \mod (\lvert\chi(i)\rvert+1))$
$\ddot{\mathcal{I}}_i^t : \lvert\ddot{I}_i^t\rvert(1-\sum_{j\in\chi(i)}\beta_{i\to j}^t)$	$\left\lfloor\frac{\lvert\ddot{I}_i^t\rvert}{\lvert\chi(i)\rvert+1}\right\rfloor + (\lvert\ddot{I}_i^t\rvert \mod (\lvert\chi(i)\rvert+1))$
$\dddot{\mathcal{S}}_i^t : \sum_{j\in\chi(i)}\lvert\ddot{S}_j^t\rvert\beta_{j\to i}^t$	$\sum_{j\in\chi(i)}\left\lfloor\frac{\lvert\ddot{S}_j^t\rvert}{\lvert\chi(j)\rvert+1}\right\rfloor$
$\dddot{\mathcal{I}}_i^t : \sum_{j\in\chi(i)}\lvert\ddot{I}_j^t\rvert\beta_{j\to i}^t$	$\sum_{j\in\chi(i)}\left\lfloor\frac{\lvert\ddot{I}_j^t\rvert}{\lvert\chi(j)\rvert+1}\right\rfloor$

Table 1. $\dot{\mathcal{S}}_i^t$: susceptible people from $\dot{S}_i^t$ that answer to distancing; $\dot{\mathcal{I}}_i^t$: infected people from $\dot{I}_i^t$ that answer to distancing; $\ddot{\mathcal{S}}_i^t$: susceptible people from $\ddot{S}_i^t$ that do not answer to distancing; $\ddot{\mathcal{I}}_i^t$: infected people from $\ddot{I}_i^t$ that do not answer to distancing; $\dddot{\mathcal{S}}_i^t$: susceptible people from adjacent vertices that do not answer to distancing; $\dddot{\mathcal{I}}_i^t$: infected people from adjacent vertices that do not answer to distancing.

Thereby, the model is updated to:

$$|I_i^t| = |I_i^{t-1}| - \varepsilon|I_i^{t-1}| + v(|\dot{X}_i^{t-1}| + |\ddot{X}_i^{t-1}|)$$
$$|S_i^t| = |S_i^{t-1}| - v(|\dot{X}_i^{t-1}| + |\ddot{X}_i^{t-1}|) + \varepsilon|I_i^{t-1}|.$$

Next, we analyze the *expected value* of $\mathbb{E}[|\dot{X}_i^{t-1}|]$ and $\mathbb{E}[|\ddot{X}_i^{t-1}|]$. The probability to occur an event Y is denoted by $\mathbb{P}\{Y\}$.

The encounters of a person who answers to social distancing are restricted to the vertex that he (she) belongs. Let $\dot{Y}_{pi}^t$ be an indicator random variable which is equal to 1 if a susceptible person $p \in \dot{S}_i^t$ meets an infected person; and it is equal to 0 otherwise. Thus, $|\dot{X}_i^t| = \sum_{p=1}^{\dot{\mathcal{S}}_i^t}\dot{Y}_{pi}^t$ for all vertex i and for all time t. The encounters of a person who does not answer to distancing can occur in his (her) own vertex or adjacent vertices. In a similar way, let $\ddot{Y}_{pi\to i}^t$ ($\ddot{Y}_{pi\to j}^t$) an indicator random variable which is equal to 1 if a susceptible person $p \in \ddot{S}_i^t$ meets an infected person in vertex i (in vertex $j \in \chi(i)$). So, $|\ddot{X}_i^t| = \sum_{p=1}^{\ddot{\mathcal{S}}_i^t}(\ddot{Y}_{pi\to i}^t) + \sum_{j\in\chi(i)}(\sum_{p=1}^{T_j}\ddot{Y}_{pi\to j}^t)$, where T_j is the number of susceptible people from i circling in $j \in \chi(i)$. In general case, $T_j = |\ddot{S}_i^t|\beta_{i\to j}^t$. Our experiments consider $T_j = \left\lfloor\frac{|\ddot{S}_i^t|}{|\chi(i)|+1}\right\rfloor$ (see Table 1).

The expected value of $|\dot{X}_i^t|$ is $\mathbb{E}[|\dot{X}_i^t|] = \mathbb{E}[\sum_{p=1}^{\dot{\mathcal{S}}_i^t}\dot{Y}_{pi}^t] = \sum_{p=1}^{\dot{\mathcal{S}}_i^t}\mathbb{E}[\dot{Y}_{pi}^t] = \sum_{p=1}^{\dot{\mathcal{S}}_i^t}\mathbb{P}\{\dot{Y}_{pi}^t\} = \dot{\mathcal{S}}_i^t\mathbb{P}\{\dot{Y}_{pi}^t\}$. Similarly, we have the expected value $\mathbb{E}[|\ddot{X}_i^t|] = \ddot{\mathcal{S}}_i^t\mathbb{P}\{\ddot{Y}_{pi\to i}^t\} + \sum_{j\in\chi(i)}T_j\mathbb{P}\{\ddot{Y}_{pi\to j}^t\}$. Note that we have to calculate the probability to occur a contact between a susceptible person $p \in \dot{S}_i^t$ and an infected person ($\mathbb{P}\{\dot{Y}_{pi}^t\}$) and the probabilities to occur a contact between a susceptible person $p \in \ddot{S}_i^t$ and an infected person ($\mathbb{P}\{\ddot{Y}_{pi\to i}^t\}$ and $\mathbb{P}\{\ddot{Y}_{pi\to j}^t\}$). Before that, let us rewrite the model in function of the expected value of susceptible and infected people over time. It is important to note that we can work with lower

and upper bounds for the expected values. These bounds can always be integer numbers (as long as they are initially integer number). Given $|I_i^{t-1}|$ and $|S_i^{t-1}|$, and given constants ε and v, the model is update to (the symbol $=:$ means *by definition*):

$$\begin{aligned}
\mathbb{E}[|I_i^t|] &= \mathbb{E}[|I_i^{t-1}| - \varepsilon|I_i^{t-1}| + v(|\dot{X}_i^{t-1}| + |\ddot{X}_i^{t-1}|)] \\
&= |I_i^{t-1}| - \varepsilon|I_i^{t-1}| + v(\mathbb{E}[|\dot{X}_i^{t-1}|] + \mathbb{E}[|\ddot{X}_i^{t-1}|]) \\
&\geq |I_i^{t-1}| - \lceil \varepsilon|I_i^{t-1}| \rceil + \lfloor v(\mathbb{E}[|\dot{X}_i^{t-1}|] + \mathbb{E}[|\ddot{X}_i^{t-1}|]) \rfloor =: |I_i^t|, \\
\mathbb{E}[|S_i^t|] &= \mathbb{E}[|S_i^{t-1}| - v(|\dot{X}_i^{t-1}| + |\ddot{X}_i^{t-1}|) + \varepsilon|I_i^{t-1}|] \\
&= |S_i^{t-1}| - v(\mathbb{E}[|\dot{X}_i^{t-1}|] + \mathbb{E}[|\ddot{X}_i^{t-1}|]) + \varepsilon|I_i^{t-1}| \\
&\leq |S_i^{t-1}| - \lfloor v(\mathbb{E}[|\dot{X}_i^{t-1}|] + \mathbb{E}[|\ddot{X}_i^{t-1}|]) \rfloor + \lceil \varepsilon|I_i^{t-1}| \rceil =: |S_i^t|.
\end{aligned}$$

The previous model uses *floor* and *ceiling* functions. Observe that, if $|I_i^{t-1}|$ and $|S_i^{t-1}|$ are integer numbers then $|I_i^t|$ and $|S_i^t|$ are also integers. Moreover, the expected value of infected (susceptible) people of vertex i and on time t is at least (at most) $|I_i^t|$ ($|S_i^t|$). Now, we describe the probabilities.

The probabilities $\mathbb{P}\{\dot{Y}_{pi}^t\}$, $\mathbb{P}\{\ddot{Y}_{pi\to i}^t\}$ *and* $\mathbb{P}\{\ddot{Y}_{pi\to j}^t\}$*:* Fixed a time t, we know that the number of infected in any vertex i is $\dot{\mathcal{I}}_i^t + \ddot{\mathcal{I}}_i^t + \dddot{\mathcal{I}}_i^t$; and we know that the total number of possible encounters (without repetition) between two people (one being susceptible) is $\dot{\mathcal{N}}_i^t + \ddot{\mathcal{N}}_i^t + \dddot{\mathcal{N}}_i^t - 1$. So, the probability of a susceptible people to be infected in any vertex i is $\mathbb{P}\{\dot{Y}_{pi}^t\} = \frac{\dot{\mathcal{I}}_i^t + \ddot{\mathcal{I}}_i^t + \dddot{\mathcal{I}}_i^t}{\dot{\mathcal{N}}_i^t + \ddot{\mathcal{N}}_i^t + \dddot{\mathcal{N}}_i^t - 1}$. Since the last probability holds for any vertex i, we have that $\mathbb{P}\{\ddot{Y}_{pi\to i}^t\} = \mathbb{P}\{\dot{Y}_{pi}^t\}$; and $\mathbb{P}\{\ddot{Y}_{pi\to j}^t\} = \mathbb{P}\{\dot{Y}_{pj}^t\}$, for all $j \in \chi(i)$. Next, we extend this proposal for SIR model.

5 The SIR model

In SIR model we have, a set of susceptible people S_i^t, a set of infected people I_i^t and a set of *recovered* people R_i^t, for each vertex i and each time t. Once again, the total people number $N_i^t = S_i^t \cup I_i^t \cup R_i^t$ is maintained constant over time. In this case, a susceptible person on time t can be infected on time $t+1$. An infected person on time t can be recovered on time $t+1$. A recovered person does not become infected again. Now, given $|I_i^{t-1}|$, $|S_i^{t-1}|$ and $|R_i^{t-1}|$, and given the constants ε and v, the model can be write as:

$$\begin{aligned}
|I_i^t| &= |I_i^{t-1}| - \varepsilon|I_i^{t-1}| + v(|\dot{X}_i^{t-1}| + |\ddot{X}_i^{t-1}|), \\
|S_i^t| &= |S_i^{t-1}| - v(|\dot{X}_i^{t-1}| + |\ddot{X}_i^{t-1}|), \\
|R_i^t| &= |R_i^{t-1}| + \varepsilon|I_i^{t-1}|,
\end{aligned}$$

where $\dot{X}_i^{t-1}$ ($\ddot{X}_i^{t-1}$) is the set of susceptible and distancing people (without distancing) of vertex i that encountered an infected person. The expected value of the number of infected people ($\mathbb{E}[|I_i^t|]$) is equal to that given in the previous

section. For the other expected values we have

$$\begin{aligned}
\mathbb{E}[|S_i^t|] &= \mathbb{E}[|S_i^{t-1}| - v(|\dot{X}_i^{t-1}| + |\ddot{X}_i^{t-1}|)] \\
&= |S_i^{t-1}| - v(\mathbb{E}[|\dot{X}_i^{t-1}|] + \mathbb{E}[|\ddot{X}_i^{t-1}|)] \\
&\leq |S_i^{t-1}| - \lfloor v(\mathbb{E}[|\dot{X}_i^{t-1}|] + \mathbb{E}[|\ddot{X}_i^{t-1}|)] \rfloor =: |S_i^t|, \\
\mathbb{E}[|R_i^t|] &= \mathbb{E}[|R_i^{t-1}| + \varepsilon |I_i^{t-1}|] \\
&= |R_i^{t-1}| + \varepsilon |I_i^{t-1}| \\
&\leq |R_i^{t-1}| + \lceil \varepsilon |I_i^{t-1}| \rceil =: |R_i^t|.
\end{aligned}$$

Once again, if $|I_i^{t-1}|$, $|S_i^{t-1}|$ and $|R_i^{t-1}|$ are integer number then $|I_i^t|$, $|S_i^t|$ and $|R_i^t|$ will also be. The expected value of infected (susceptible, recovered) people of vertex i and on time t is at least (at most, at most) $|I_i^t|$ ($|S_i^t|$, $|R_i^{t-1}|$).

In SIR model simulations, the social distancing factor is applied on sets S_i^t, I_i^t and R_i^t of the following way: $|\dot{S}_i^t| = \lfloor \alpha_i^t |S_i^t| \rfloor$, $|\ddot{S}_i^t| = |S_i^t| - |\dot{S}_i^t|$, $|\dot{I}_i^t| = \lfloor \alpha_i^t |I_i^t| \rfloor$, $|\ddot{I}_i^t| = |I_i^t| - |\dot{I}_i^t|$ and $|\dot{R}_i^t| = \lfloor \alpha_i^t |R_i^t| \rfloor$, $|\ddot{R}_i^t| = |R_i^t| - |\dot{R}_i^t|$. The set of people that answer to distancing is $\dot{N}_i^t = \dot{S}_i^t \cup \dot{I}_i^t \cup \dot{R}_i^t$ and the set of people that do not is $\ddot{N}_i^t = \ddot{S}_i^t \cup \ddot{I}_i^t \cup \ddot{R}_i^t$. All variables from Table 1 still apply, and the Table 2 shows the variables representing recovered people that also circulate in vertex i.

General case	Experiment case
$\dot{\mathcal{R}}_i^t : \lambda_{\dot{R}} \lvert \dot{R}_i^t \rvert$	$\lfloor \lambda_{\dot{R}} \lvert \dot{R}_i^t \rvert \rfloor$
$\ddot{\mathcal{R}}_i^t : \lvert \ddot{R}_i^t \rvert (1 - \sum_{j \in \chi(i)} \beta_{i \to j}^t)$	$\left\lfloor \frac{\lvert \ddot{R}_i^t \rvert}{\lvert \chi(i) \rvert + 1} \right\rfloor + (\lvert \ddot{R}_i^t \rvert \mod (\lvert \chi(i) \rvert + 1))$
$\dddot{\mathcal{R}}_i^t : \sum_{j \in \chi(i)} \lvert \ddot{R}_j^t \rvert \beta_{j \to i}^t$	$\sum_{j \in \chi(i)} \left\lfloor \frac{\lvert \ddot{R}_j^t \rvert}{\lvert \chi(j) \rvert + 1} \right\rfloor$

Table 2. $\dot{\mathcal{R}}_i^t$: recovered people from $\dot{R}_i^t$ that answer to distancing; $\ddot{\mathcal{R}}_i^t$: recovered people from $\ddot{R}_i^t$ that do not answer to distancing; $\dddot{\mathcal{R}}_i^t$: recovered people from adjacent vertices that do not answer to distancing.

Now, we denote the total of people circling in vertex i by $\dot{\mathcal{N}}_i^t + \ddot{\mathcal{N}}_i^t + \dddot{\mathcal{N}}_i^t$ where $\dot{\mathcal{N}}_i^t = \dot{\mathcal{S}}_i^t + \dot{\mathcal{I}}_i^t + \dot{\mathcal{R}}_i^t$, $\ddot{\mathcal{N}}_i^t = \ddot{\mathcal{S}}_i^t + \ddot{\mathcal{I}}_i^t + \ddot{\mathcal{R}}_i^t$ and $\dddot{\mathcal{N}}_i^t = \dddot{\mathcal{S}}_i^t + \dddot{\mathcal{I}}_i^t + \dddot{\mathcal{R}}_i^t$. The encounters of a susceptible person and an infected and the probabilities of these events still hold. Next, we describe the results obtained for some network topologies.

6 SIR model simulations: results and analysis

In this section we describe the experiments performed on different *network topologies*. For us, network topology is the way how the network connections are organized and how they define a structure (if any). Our motivation for these experimental analysis is that the topologies analyzed and real world topologies (i.e. the way how the neighborhoods, cities, etc, are connected) can have similarity. For a case of extreme necessity, some topology could by applied in practice (and in emergency way), changing temporarily the usual network connections.

The topologies analyzed were the following: *cyclical*, *star*, *wheel*, *complete*, *line* and *grid*. All these topologies are *planar networks* unless the complete topology. We illustrate each one of them in Fig. 1.

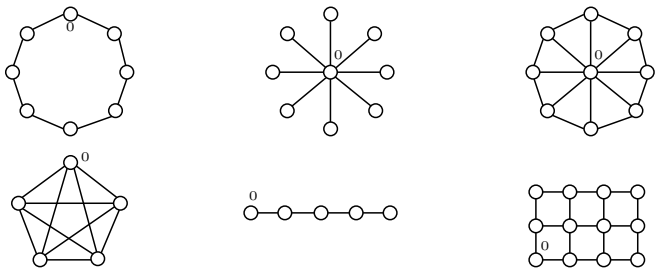

Fig. 1. The cyclical, star, wheel, complete, line and grid topologies.

Next, we show some characteristic graphics for the SIR model ($t \times n$ where t represents a day from 0 up to 200 and n represents the number of susceptible, infected or recovered people). The graphics in Fig. 2 correspond to the total number of susceptible, infected and recovered people on the wheel, star, grid, cyclical and complete topologies. The first scenario did not consider social distancing ($\alpha_i^t = 0$ for all i and all t). Each topology has 100 vertices and each vertex i has $N_i^t = 3000$ people. Initially, all topologies have 400 infected (in vertex labeled 0 in Fig. 1). When this is not the case, we explicitly describe for which topology this value was changed. All other people are initially susceptible and there is no recovered people. The daily recovered rate and the daily virulence rate are respectively $\varepsilon = \frac{29}{200}$ and $v = \frac{91}{200}$. Such rates have been recently used and they are related to the COVID-19 disease (see, for example, in [2]). The line topology results were similar to cyclical topology: low number of infected people, almost constant over time and a long plateau. The curves of susceptible and recovered people for the line case were less steep. The characteristic curves to SIR model did not appear for the complete topology (400 infected). In this case, the number of people circling each vertex was not enough to increase the expected value of infected people. However, raising the initially infected number to 500 for complete topology, the infection spreads (in Fig. 2 bottom middle graphic). Observe that the minimum number of susceptible and the maximum number of recovered for all experiments without social distancing are very similar: mean of approximately 15024 for susceptible and 284976 for recovered. So, almost all people were infected for all topologies in this case. However, the peak of infected for cyclical (grid) is almost 83.5% (33%) lower than the highest peak from star topology.

The social distancing was considered for the experiments illustrated in Fig.2 (bottom right graphic) and Fig. 3 (top graphics). The people that do answer to social distancing but still circulate in their vertex (for some unavoidable reason)

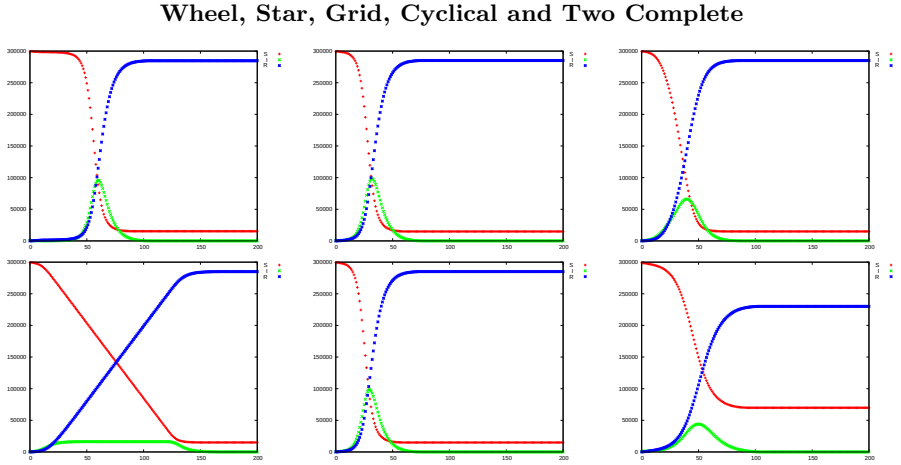

Fig. 2. Graphics without social distancing unless the bottom right graphic.

are $\lambda_{\dot{S}} = \frac{2}{5}$, $\lambda_{\dot{I}} = \frac{1}{10}$ and $\lambda_{\dot{R}} = \frac{3}{5}$. The constants ε and v are the same as previous. Moreover, the social distancing considered over time was constant in $\alpha_i^t = \frac{2}{5}$ for all i and all t (40% of people do answer to social distancing). Once again, each vertex has 3000 people and a single vertex has 400 infected people. The distancing in these conditions was enough to control the infection spreading on star, wheel and complete topologies. For the complete topology and when the initially number of infected people is 1000, we obtain the bottom right graphic in Fig. 2. Compare this same graphic with the graphic to its left in Fig. 2 (complete without social distancing). We can clearly note the gain that the social distancing can provide in a dense network whose initially infected people are twice bigger. For the cyclical (top right graphic in Fig. 3) and line (not shown), the curve for infected people was lower than the same topologies without social distancing. For the grid topology (top left in Fig. 3), the peak of infected was nearly 58% lower (and smoother) than the peak from the grid topology without social distancing (the top right graphic in Fig. 2). To conclude, the graphics in Fig. 3 (bottom) illustrate a periodical social distancing case applied to grid and complete topology (the last, initially 1000 infected people). In the begin of the period, there is no social distancing factor. Over time, the social distancing factor gradually increases until to reach the peak (day five) with distancing factor in 70%. After, the distancing factor starts to gradually decrease until to cancel the factor (day ten). This behavior repeats over time. In this case, the results show expected zigzag lines. The peak of infected from grid topology with periodic distancing was 62% lower than the same topology without distancing and, for the complete topology case, 61% lower. Therefore, the performed simulations suggest that, given the previous initial conditions, the social distancing, and cyclical, line and grid topologies can decrease the peak of infected people during the spreading of a disease, one of the measures that we consider important.

Top: Grid and Cyclical; Bottom: Grid and Complete

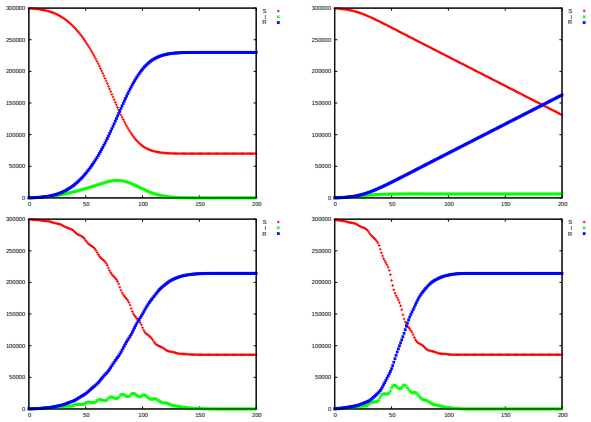

Fig. 3. Top: Social distancing in 40% over time. On the right, the curves continue its trajectory although the interruption on time 200. **Bottom:** Social distancing given by a periodical function (sine module function). The function period is ten days. The peak occurs on day five and corresponds to factor social distancing equal to 70%

References

1. Ahmed, E., Agiza, H.N.: On modeling epidemics including latency, incubation and variable susceptibility. Physica A: Stat. Mech. and its App. **253**(1-4), 347–352 (1998)
2. Bastos, S.B., Cajueiro, D.O.: Modeling and forecasting the Covid-19 pandemic in Brazil. arXiv preprint arXiv:2003.14288 (2020)
3. Beauchemin, C., Samuel, J., Tuszynski, J.: A simple cellular automaton model for influenza A viral infections. Journal of Theoretical Biology **232**(2), 223–234 (2005)
4. Fitzpatrick, J., DeSalvo, K.: Helping public health officials combat COVID-19, available at `https://www.blog.google/technology/health/covid-19-community-mobility-reports?hl=en`
5. Hethcote, H.W.: Three basic epidemiological models. In: Applied Mathematical Ecology, pp. 119–144. Springer (1989)
6. Kermack, W.O., McKendrick, A.G.: A contribution to the mathematical theory of epidemics. Proc. of the Acad. Roy. Sci. of London. Series A **115**(772), 700–721 (1927)
7. Linge, S., Langtangen, H.P.: Programming for computations-MATLAB/Octave. Springer Nature (2016)
8. Ramani, A., Carstea, A.S., Willox, R., Grammaticos, B.: Oscillating epidemics: a discrete-time model. Physica A: Stat. Mech. and its App. **333**, 278–292 (2004)
9. Tomassini, M.: Generalized automata networks. In: International Conference on Cellular Automata. pp. 14–28. Springer (2006)
10. White, S.H., Del Rey, A.M., Sánchez, G.R.: Modeling epidemics using cellular automata. Applied Mathematics and Computation **186**(1), 193–202 (2007)
11. Willox, R., Grammaticos, B., Carstea, A.S., Ramani, A.: Epidemic dynamics: discrete-time and cellular automaton models. Physica A: Stat. Mech. and its App. **328**(1-2), 13–22 (2003)